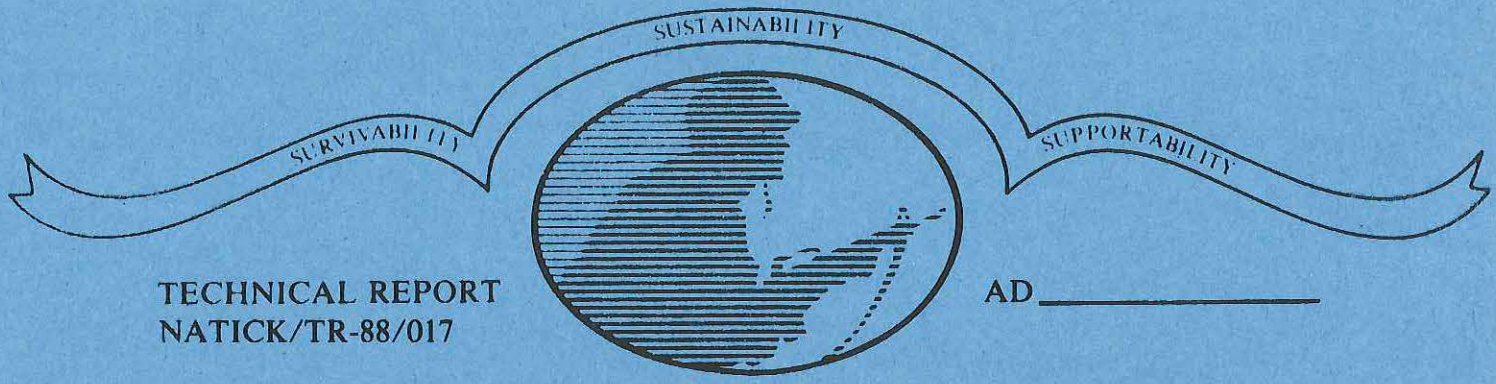

TECHNICAL REPORT
NATICK/TR-88/017

AD_____

PHYSICAL PARAMETERS AFFECTING LIQUID PENETRATION AND WETTING OF FABRICS

BY

RONALD SEGARS
ERNEST JOHNSON
LANDA HOKE
CEDRIC BUETTNER
BRIAN PANGRLE
DAVID NORDQUIST

FINAL REPORT JUNE 1987

FOR THE PERIOD
APRIL 1984 – OCTOBER 1986

UNITED STATES ARMY NATICK
RESEARCH, DEVELOPMENT AND ENGINEERING CENTER
NATICK, MASSACHUSETTS 01760-5000

SCIENCE AND ADVANCED TECHNOLOGY DIRECTORATE

DISCLAIMERS

The findings contained in this report are not to be construed as an official Department of the Army position unless so designated by other authorized documents.

Citation of trade names in this report does not constitute an official endorsement or approval of the use of such items.

DESTRUCTION NOTICE

For Classified Documents:

Follow the procedures in DoD 5200.22-M, Industrial Security Manual, Section II-19 or DoD 5200.1-R, Information Security Program Regulation, Chapter IX.

For Unclassified/Limited Distribution Documents:

Destroy by any method that prevents disclosure of contents or reconstruction of the document.

REPORT DOCUMENTATION PAGE

Form Approved OMB No. 0704-0188

1a. REPORT SECURITY CLASSIFICATION UNCLASSIFIED	1b. RESTRICTIVE MARKINGS
2a. SECURITY CLASSIFICATION AUTHORITY	3. DISTRIBUTION/AVAILABILITY OF REPORT Approved for public release; distribution unlimited.
2b. DECLASSIFICATION/DOWNGRADING SCHEDULE	
4. PERFORMING ORGANIZATION REPORT NUMBER(S) NATICK/TR-88/017	5. MONITORING ORGANIZATION REPORT NUMBER(S)
6a. NAME OF PERFORMING ORGANIZATION U.S. Army Natick RD&E Center Biochem Br, BioSD, SATD 6b. OFFICE SYMBOL (If applicable) STRNC-YMB	7a. NAME OF MONITORING ORGANIZATION
6c. ADDRESS (City, State, and ZIP Code) Kansas Street Natick, MA 01760-5020	7b. ADDRESS (City, State, and ZIP Code)
8a. NAME OF FUNDING/SPONSORING ORGANIZATION 8b. OFFICE SYMBOL (If applicable)	9. PROCUREMENT INSTRUMENT IDENTIFICATION NUMBER
8c. ADDRESS (City, State, and ZIP Code)	10. SOURCE OF FUNDING NUMBERS PROGRAM ELEMENT NO. 61101A; PROJECT NO. A91A; TASK NO. 07; WORK UNIT ACCESSION NO. DA304503

11. TITLE (Include Security Classification)

(U) Physical Parameters Affecting Liquid Penetration and Wetting of Fabrics

12. PERSONAL AUTHOR(S) SEGARS, Ronald; Johnson, Ernest; Hoke, Landa; Buettner, Cedric; Prangrle, Brian; and Nordquist, David

13a. TYPE OF REPORT	13b. TIME COVERED	14. DATE OF REPORT (Year, Month, Day)	15. PAGE COUNT
Final	FROM 04/84 TO 10/86	1987 June	49

16. SUPPLEMENTARY NOTATION

17. COSATI CODES			18. SUBJECT TERMS (Continue on reverse if necessary and identify by block number)		
FIELD	GROUP	SUB-GROUP	Fabrics	Wetting	Roughness
			Contact Angle	Liquid Penetration	
			Surface Tension	Critical Surface Tension	

19. ABSTRACT (Continue on reverse if necessary and identify by block number)

The purpose of this research is the development and evaluation of a test procedure for determining the water repellency of films and fabrics of military interest. The approach selected has been used by several investigators. The method determines the critical surface tension (γ_c) of the material by measuring the angle of contact between the fabric and a series of liquids of different surface tensions. A camera-microscope system is used to obtain the contact angles. Young's equation and theoretical equations proposed by other researchers are used to analyze test results. Data obtained on several experimental films was analyzed using the approaches of Fowkes and Good. For practical purposes both approaches gave similar results. However, analysis of data reveals a fundamental limitation of the method. When applied to materials of low surface energy, particularly the rough surface of a water repellent woven fabric, a long extrapolation is required to obtain γ_c. Since the exact relationship between contact angle and the surface tension is still unknnown, long extrapolation cannot be used to obtain reliable γ_c data. Although this method of

(CONTINUED OTHER SIDE)

20. DISTRIBUTION/AVAILABILITY OF ABSTRACT	21. ABSTRACT SECURITY CLASSIFICATION	
☒ UNCLASSIFIED/UNLIMITED ☐ SAME AS RPT. ☐ DTIC USERS	UNCLASSIFIED	
22a. NAME OF RESPONSIBLE INDIVIDUAL RONALD SEGARS	22b. TELEPHONE (Include Area Code) (617)651-4550	22c. OFFICE SYMBOL STRNC-YMB

DD Form 1473, JUN 86 *Previous editions are obsolete.* SECURITY CLASSIFICATION OF THIS PAGE
UNCLASSIFIED

19. ABSTRACT (Continued)

characterizing the wettability of surfaces has been widely used, it appears that other approaches are needed for evaluating the wettability of highly repellent rough surfaces.

PREFACE

This report describes research performed during 1984-1986, under Project #1L161101A91A07139.

TABLE OF CONTENTS

LIST OF FIGURES

LIST OF TABLES

Physical Parameters Affecting Liquid Penetration and Wetting of Fabrics

INTRODUCTION

Understanding the mass transfer of liquids in fabrics is of paramount importance to the testing and development of protective clothing for military personnel. How droplets of water or potentially toxic liquids behave when placed on a fabric surface; how they spread, wet, and ultimately penetrate the fabric; how fabrics can be asymmetrical in their liquid and vapor transport properties--all are questions that must be answered before the optimum protective suit becomes a reality.

Tests that study the behavior of water and other liquids (under static or simulated rainfall conditions) are critical to understanding liquid transfer in fabrics. This information will provide the basis for engineering know-how to optimize the asymmetric transport properties of protective breathable fabrics. These accomplishments will come only with extensive experimental and theoretical efforts that study (both individually and in concert) the physical mechanisms involved in the wetting of fabrics.

These efforts have been ongoing for many years and include both theoretical and experimental studies. Zisman and coworkers (1),(2),(3) through extensive experimental work introduced the concept of critical surface tension γ_c and provided a means of quantifying the wettability of a solid surface. Their plots of $\cos \theta$ vs γ have provided a measure of the wetting potential of many polymer surfaces. Good and coworkers (4),(5),(6) investigated the nature of interactions at the interface between a solid and a liquid. Based on the Berthelot relation for the

attractive constants between like and unlike molecules, they proposed a modified geometric mean representation for the total interaction force and introduced the ϕ function. This system dependent function was determined from known or separately measured molecular parameters of the system. Fowkes (7),(8) provided additional information on the nature of these interactions, focussing primarily on the dispersion components. He used the geometric mean relationship proposed by Good to derive his dispersion force equation and showed that the dispersion component of the surface tension was essentially Zisman's γ_c. Owens and Wendt (9) added a term to the Fowkes equation to account for the polar forces. This added term was also based on the geometric mean. Saito and Yabe (1Ø) used this extended Fowkes equation to evaluate the dispersion and polar components of several polymer films. Data on polystyrene and polyethylene showed that the pair of liquids chosen to provide the contact angle data necessary to solve the equation had a significant effect on the results obtained. For this study, the liquid pair giving results closest to the average for all pairs tested (twelve) was used to evaluate the remaining polymer films. Other investigators have studied the use of a harmonic mean approximation for one or both of the interaction terms. Wu (11), through theoretical and experimental studies on polymer systems concluded that the harmonic mean should be used for the dispersion component of the interaction force when the polarizability of the two phases is approximately equal. For the polar component, he found empirically that the harmonic mean gave better results even though the geometric mean might be preferred theoretically. In studies on copolymer hydrogels, Yuk and Jhon (12) used the geometric mean for the dispersion component of the interaction force and the harmonic mean for the polar component to show

contact angle variation due to surface deformation. However, no comparison was made between the chosen model and other models for the interaction forces.

Considerable work has been done to quantify the effect of surface roughness on the measurement of contact angle. Dettre and Johnson (13), Oliver and Mason (14) and others (15),(16),(17),(18) have shown that surface roughness has a significant effect on the measurement of contact angle and the spreading of liquids on surfaces and is one of the factors responsible for contact angle hysteresis. At present, no universally accepted method has been established for obtaining and analyzing contact angle data on rough surfaces.

A recent review article by de Gennes (19) attempts to integrate all of these factors into a unified picture of the wetting of surfaces. His paper discusses the measurement and interpretation of contact angles and their relation to the wettability or wetting of materials, the effect of contact angle hysteresis, and other factors on the spreading of liquid drops. He concluded that the spreading of nonvolatile, nonwetting liquids (dry spreading) is reasonably well understood and that spreading behavior is consistent with theory. On the other hand, the equilibrium spreading behavior of wetting liquids (moist spreading) depends on the relative availability of the saturated vapor. Thus, an additional parameter is required and the solutions are no longer unique.

The main focus of this study was the development of objective methods to measure the surface properties of fabrics and films and to relate these measurements to the actual wetting and penetration of the materials. The ultimate goal of the work is to develop an experimental-theoretical model

that will not only predict the wetting behavior of experimental fabrics but will also allow the design of fabrics with optimum properties for particular applications.

MATERIALS AND METHODS

Fabrics

Samples of experimental low surface energy films were obtained from the Fiber & Fabric Technology Branch of the Individual Protection Directorate (IPD). These materials, identified by trade name or by fabric and coating identifiers, were evaluated by the test procedures established during this research effort, and are listed in Table 1.

TABLE 1. Experimental Films Submitted for Evaluation of Surface Properties

	TRADE NAME	FABRIC DESCRIPTION	VEE#
1.	Bioflex	(Silicone rubber)/knitted nylon	5339
2.	Dinkam 3501S	(Amino Acid polymer)/nylon	5340
3.	Dinkam 3001	(Amino Acid)/nylon	5341
4.	Dinkam PF 151	(Amino Acid)/nylon	5342
5.	Klimate	(PTFE)/Nyco fabric	5381
6.	Gore-Tex(R) II	(PTFE)/Nyco fabric	5382
7.	Bion II	(Polyurethane elastomer)/Nyco (no finish)	5383
8.	Klimate	(PTFE)/Nyco (no finish)	5384
9.	Porelle film	(Co-polyester/polyurethane film)	5385
10.	Sympatex/NYCO	(Co-polyether/polyester film)/NYCO	5479

In addition to these experimental films, IPD submitted for evaluation several fabrics which were treated with a water resistant material or were laminated with a water resistant layer included. These fabrics and the coating or laminate identifiers are listed in Table 2.

TABLE 2. Combat Uniform Fabrics Submitted for Evaluation of Surface Properties

ITEM	DESCRIPTION
1.	7 oz. Nyco, Quarpel treated
2.	Stormshed
3.	5 oz. Nyco/Gore-Tex II
4.	5 oz. Nyco/Gore-Tex II/SAR/taffeta
5.	Stormshed/SAR/taffeta
6.	7 oz. Nyco, Q-treated/50-mil foam
7.	7 oz. Nyco, Q-treated/70-mil foam
8.	7 oz. Nyco, Q-treated/SAR/taffeta

Items 2 and 5 not evaluated due to problems with surface roughness.
Items 3 and 4 drops spread within 30 seconds.
Items 6, 7, and 8 surface similar to item 1.

Liquids for Contact Angle Measurement

A series of liquids formed by varying the concentration of ethanol in ethanol-water mixtures was selected for use in determining contact angles following the work of Cowsar & Speaker (20). This series of liquids is both polar and hydrogen bonding and should give larger contact angles than liquids from the non-polar and non-hydrogen bonding series. Dann (21), (22) gives the polar and dispersion components of surface tension for this series of liquids. The ethanol-water series was chosen because it includes water, the liquid of primary importance in this work, even though this series does not represent the most severe test of wetting resistance. Several concentrations were made from 190 proof ethyl alcohol and distilled water. The surface tension of each concentration was taken from Dann and is given in Table 3. Data were fitted to a semi-log plot, Fig. 1, to permit interpolation of surface tension values at concentrations not listed in the report; interpolated data are enclosed in parentheses in Table 3. Several checks of the surface tension values were made as described later, but the published values given in Table 3 and Fig. 1 were used in this work.

TABLE 3. Surface Tension of Ethanol-Water Mixtures

% ETHANOL	SURFACE TENSION NEWTON/cm*10^{5}
0	72.2
10	51.3
20	(42.1)
30	36.1
40	(32.5)
50	30.0
60	28.0
70	27.2
80	25.6
90	24.0
100	(23.1)

Data from Dann, 1970.

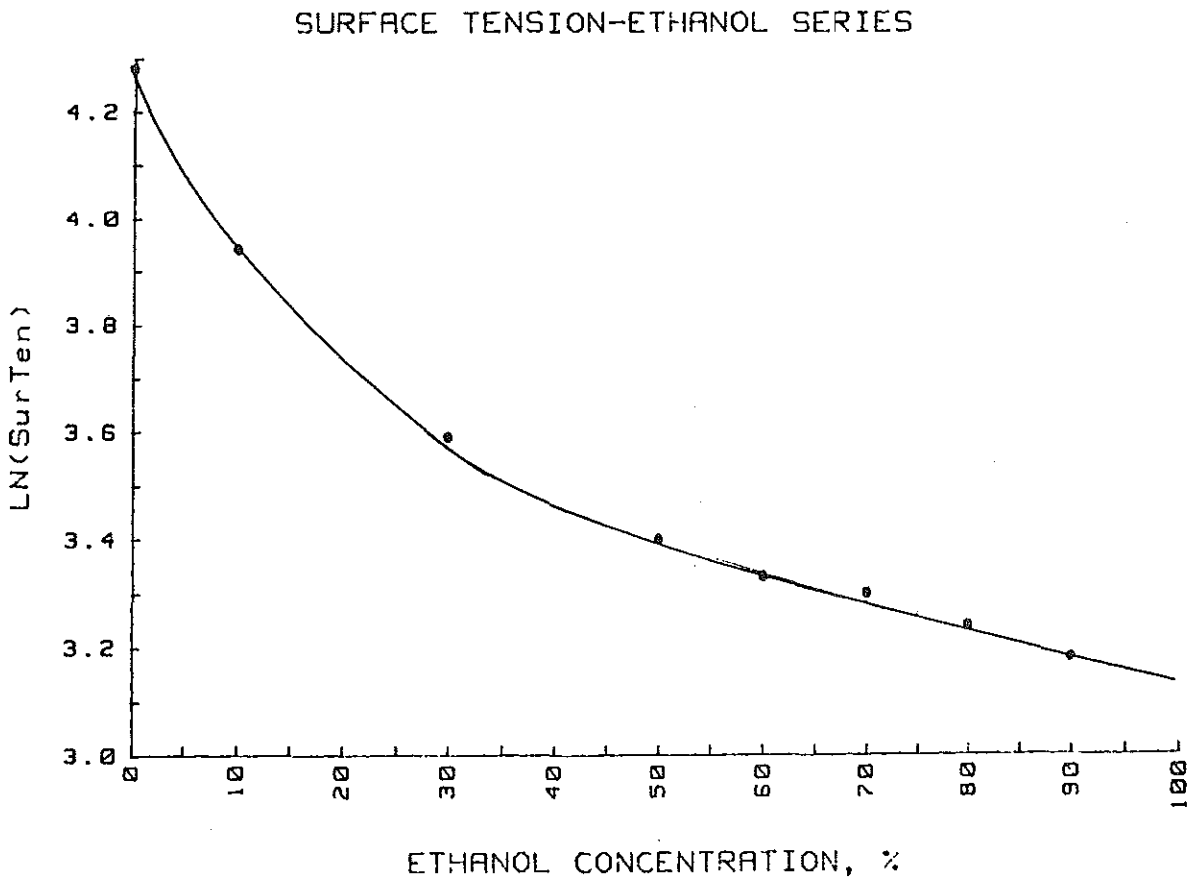

Figure 1. The natural log of surface tension plotted vs ethanol concentration

Source: Dann 1970, Parts I and II.

General Approach

The method selected for the evaluation of the surface properties of fabrics and films follows the approach first proposed by Fox and Zisman (2) in 1950. This approach determines the critical surface tension γ_c of a fabric by measuring the contact angle θ between a liquid drop and the fabric (Fig. 2). γ_c is a measure of the free energy of the surface and is numerically equal to the surface tension of that liquid which just completely wets the surface of the fabric, i.e., a liquid that forms a contact angle of 0° with the fabric. In general, it is believed that this is strictly true where only dispersion forces are in effect (7),(8). If other forces come into play, the value obtained may not be the true free energy of the surface but it is still expected to be a good practical measure of its liquid repellency (19).

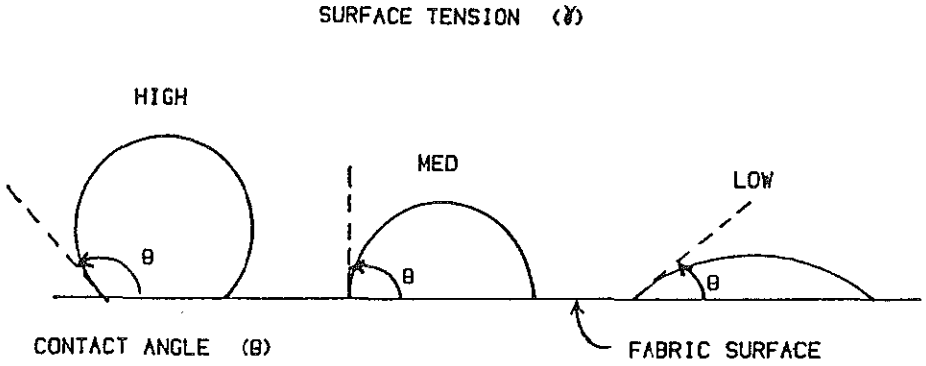

Figure 2. Schematic diagram showing the contact angle θ for high, medium and low surface tension liquids on a smooth surface.

The goal of this effort was to develop a rapid, convenient method to evaluate the water repellency of military fabrics. The precautions often taken in the measurement of contact angles (system equilibrium, measurement of advancing and receding angles, temperature control, etc.) were not consistent with the above goals. For this reason, specific procedures were developed.

Measurement of Contact Angle

The above approach to the determination of the critical surface tension requires the measurement of the contact angle θ for a series of liquids of differing surface tensions. To streamline the process of obtaining the contact angle measurements, it was decided to place five or six drops on the fabric surface and take a single photograph of the drops for the various liquids. This idea had several serious drawbacks. Ideally the photograph would be taken only after the drops had reached equilibrium. However, all the drops could not be deposited simultaneously and since we were not attempting to get complete equilibrium, evaporation, adsorption, and other factors made time a critical element, especially for the liquids of the lower surface tensions. Another difficulty with the multiple drop method was the problem of camera focussing. The drop image had to be in very sharp focus because the photo of the drop had to be enlarged about 40 times to get the required accuracy. When the drops are placed on the fabric they tend to move toward areas of higher free surface energy. To obtain the required sharpness of image, experience showed that each drop had to be brought into focus individually. A 35-mm camera, which was equipped with a bellows extension to provide a magnification of about 10X on 35-mm slide film, satisfied these requirements.

The method did not work well with liquids of low surface tension where some spreading occurred before the picture was taken. It was decided to keep the deposition time constant at a value just long enough to assure that the dynamic effects of depositing the drop had vanished. This required that the camera be prefocussed on the exact spot where the drop would be placed. A microscope with a camera attachment provided about the same magnification as the bellows camera and had a greater depth of field. This made the focus less critical and permitted the necessary prefocussing.

A modification of this third method was developed to address some of the problems associated with surface roughness. In general, the systematic roughness of the fabrics made it quite likely that the contact angles in mutually perpendicular directions, i.e., parallel and perpendicular to the yarn orientation, would be different. It was believed that the contact angle both parallel and perpendicular to the fiber axis should be measured. A rotating stage from a microscope was placed directly below the location where the drop was to be placed. By mounting the dispensing syringe on a biaxial positioner, it was possible to place the drop on the axis of rotation of the stage. Thus the camera axis could be aligned parallel to the fiber axis, the camera focussed, and the picture taken. The stage could then be rotated 90^{o} and a second picture representing the view perpendicular to the fiber axis taken without refocussing. This system worked very well for all except the most rapidly spreading liquids for which any contact angle data is questionable.

Enlargement of the Drop Image

The deposited drops were enlarged about 40X, usually in two steps, starting with the 10X magnification of the camera-bellows system or the microscope-camera unit. The drop image on the 35-mm slides was further enlarged to an overall drop magnification of about 40X by photographing the image through a Zeiss light microscope and providing an enlarged copy on polaroid film. A second method utilized a two-dimensional measuring microscope to record the drop contour from the 35-mm slide. This method was time-consuming but provided much detail concerning the exact shape of the drop. A third method, which was used for most of the measurements, projected the photographed image of the drop onto a screen where drop height and width or the contact angles could be measured directly. All three methods provided accurate values for the contact angle.

Lighting

Lighting of the drop also proved a difficult task. The drop should be shown in profile which suggests back lighting. However, with this approach, the internal surfaces of the drop often reflected the light, making bright spots or glare which blotted out the regions where data points were needed. Often several photographs in a series could not be used for data because glare made scaling of the data uncertain. Lighting from the top, the sides, the front and various combinations were tried but all have the same drawbacks due to internal and perhaps external reflection of the incident light. Indirect lighting is probably best but with the small aperture required for the large depth of field, the light must be quite intense to give adequate exposure. Long exposure times are to be avoided due to vibration, shifting, and shrinking of the drop, all

of which cause blurring of the image. For most of the work, front lighting with a directional reflector behind the drop to focus the reflected light back onto the drop was used. With this system some glare occurred but almost all photographs could be used.

Diffraction

Ideally the drop should be photographed at zero or near zero angle above the horizontal plane. Greater angles tend to distort the silhouette of the drop and could cause error in the measurement of drop height or in the direct measurement of the contact angle. But when viewed from these low inclinations, diffraction from the rough front edge of the cut fabric blurs the line of contact between the drop and the fabric. The fabric was placed on a cylindrical surface whose axis was perpendicular to the camera axis. The diameter of the cylinder, or of the cloth on the cylinder was approximately 5 cm. This makes the radius of curvature much greater than the dimensions of the drop, i.e., the surface appears flat with respect to the drop. Using the curved surface eliminated the problem of diffraction without distorting the drop profile.

Calculation of Contact Angle (θ)

The image of the original drop enlarged on a Zeiss light microscope or by projection on a screen, as described above, was measured with a straight edge ruler to determine the height of the drop, h, and the width of the drop, w, at the contact line between the drop and the fabric. The contact angle was then calculated from the equation

$$\tan(\theta/2) = 2h/w \qquad (1)$$

which assumes that the drop surface forms part of a sphere.

For some preliminary studies, the 35-mm slide was placed on the table of a measuring microscope and the entire contour of the drop image was measured. The coordinates of the drop surface near the contact point were least squares fit to a quadratic equation and the slope of the best fit line compared to other measures of the contact angle. The drop coordinates were also replotted and a circle drawn through the points using a drafting compass to check the assumption of sphericity. In most cases for drops with a contact angle greater than 90° the actual contour deviated from the true circle only near the contact region. It appeared that the effects of gravity pulled the drop down or spread the drop out and made the contact angle greater than it would be for the true sphere. However, this effect is quite small and in fact when the calculated contact angles are compared to the actually measured values obtained by drawing tangents to the drop contour at the point of contact with the fabric, the measured values are usually smaller. In most cases the values agree within about 5%. The fact that the measured values are smaller than the calculated values (when comparison to a true sphere indicates that they should be larger) is probably due to the placement of the tangent lines and the fact that there is really no "linear" region to guide their location. It is truly the tangent at a point on a curve.

Which of the three measures of contact angles best represents the true contact angle is difficult to determine. All three measures are plagued by factors which cannot be easily controlled or accurately measured. If gravity is causing a "squashing" of the lower half of the drop, both the directly measured Θ and that calculated from drop height and contact width data have this error built in. Only the best fit sphere would represent

the actual situation in the absence of gravity. If, however, the spreading pressure produces this deviation from sphericity near the contact points, only the directly measured θ's represent the true value. Fortunately, the errors involved are only on the order of 5% and are probably even less for contact angles below 90°.

Measurement of Surface Tension

The surface tension or surface free energy results from unbalanced forces on the molecules in the surface layer. These surface molecules, unlike the completely surrounded equipotential molecules that experience equal forces in all directions, have one side exposed. The unpaired electronic attractions on the free side of the molecule produce forces in the plane of the surface. The surface formed assumes a shape which minimizes these surface forces. Any enlargement of this equilibrium surface requires molecules to be brought from the interior of the liquid to the surface, and this requires the addition of energy. In practice, these surface tensions can be measured by determining the forces required to rupture a surface of known length. Measuring the force F required to lift a rod of length L from the surface of a liquid of surface tension allows the calculation of the surface tension from the equation

$$\gamma = F/2L \tag{2}$$

A sensitive displacement transducer (LVDT) was used to measure the extension of a small Ni-Span-C coil spring of spring constant k = 1 g/mm from which was suspended a 10-cm long brass rod. The rod was suspended from fine wires in such a way that its axis lay in the horizontal plane.

The output from the LVDT was fed to a stripchart recorder calibrated to read the force on the spring. Normal operating range was Ø.5 g full scale. This rod was immersed in the liquid whose surface tension was to be measured and then slowly and smoothly withdrawn. The force required to withdraw the horizontal rod was continuously monitored by the LVDT and the strip chart recorder.

The smooth and continuous withdrawal of the rod from the liquid required special consideration. Any vibration or unsteadiness in the mechanism could cause premature rupture of the fragile liquid film. The liquid to be measured was placed in an aluminum pan which in turn was set on an expanded polyurethane "float". The float was placed in a larger flat container filled with water. The float was held away from the walls of the container by guide lines attached to the float and to the outer vessel. When water was drained from the vessel at a rate preselected by adjusting a clamp on the outlet hose, the float was lowered and the brass rod withdrawn from the liquid in a well controlled manner. This system worked well for checking the surface tension values of several liquids, including those of the ethanol-water series used in this work. However, the method required about 2ØØ mL of liquid because the 1Ø cm long rod (with ends turned down to eliminate end effects) used to pull the liquid had to float freely on the surface. When shorter rods were used to measure the surface tension of solutions, which were made in 2Ø-mL quantities, the loss in sensitivity reduced the accuracy of the measurement of γ and prevented the detection of changes in γ with time due to evaporation or other factors. It was decided that more extensive measurements of the surface tension of the liquids should be postponed

until more sensitive equipment, e.g., a Cahn Electrobalance, could be purchased. For the work presented here, literature values for the surface tension of the ethanol-water series of liquids were used. These values are given in Table 1.

RESULTS AND DISCUSSION

Theoretical Considerations

The theoretical basis for the above approach lies in Young's equation (2) which can be written as

$$\cos \Theta = (\gamma_{sv} - \gamma_{sl})/\gamma_{lv} \tag{3}$$

where γ_{sv} is the surface tension of the solid when in equilibrium with the vapor of the liquid, γ_{sl} is the surface tension of the solid when in equilibrium with the liquid, and γ_{lv} is the surface tension of the liquid in equilibrium with its vapor, i.e., the measured surface tension of the liquid.

Defining the condition of complete wetting or instantaneous wetting as the point where the contact angle becomes zero, or its equivalent $\cos \Theta = 1$, we have

$$\gamma_{sv} - \gamma_{sl} = \gamma_{lv} \tag{4}$$

The significance of this equation is seen when γ_{sv} is considered as the surface tension of a solid when covered with an adsorbed film of liquid of film pressure π_e. Then

$$\gamma_{sv} = \gamma_s - \pi_e \tag{5}$$

where γ_s is the surface tension of the solid surface when exposed to dry air.

Following the reasoning of Fowkes (8) it is concluded that π_e is negligible for systems where $\gamma_s < \gamma_l$, i.e, for contact angles >0, since under these conditions attractions are stronger between liquid and vapor than between vapor and the solid. Otherwise a stable equilibrium could not exist. The conclusion that $\pi_e \simeq 0$ was reached experimentally by Graham (23),(24) Wade and Whalen (25), and Whalen (26). The theoretical work of Good (27) predicts a negligible spreading pressure of water on polyethylene of $3*10^{-5}$ ergs/cm^2 and on Teflon of $2.5*10^{-6}$ ergs/cm^2. Both values are orders of magnitude below the level of concern for our purposes and suggest that π_e can be neglected in the systems evaluated in this report.

We now consider the γ_{sl} term. A model proposed by Fowkes (7),(8) assumes that the forces acting across the interface between a liquid and a solid (or between two liquids) are primarily dispersion forces (van der Waals forces) and that the magnitude of these interactions is given by the geometric mean of the dispersion force attractions. In the interface region, there is the tension produced by the pull of the bulk liquid, γ_l, which is opposed by the attraction of the van der Waals (primarily

London) forces between the liquid and solid $\sqrt{\gamma_l^d \gamma_s^d}$. (In this discussion we follow the standard notation. The superscripts d and p represent the contributions from the dispersion and polar forces, respectively. The subscript 1 referes to the liquid and the subscript s refers to the solid, or in general, to the substrate on which liquid 1 is placed). The sum of these two forces is then $\gamma_l - \sqrt{\gamma_l^d \gamma_s^d}$. Considering the solid, it produces tensions in the interface region of γ_s due to the bulk solid and of $\sqrt{\gamma_s^d \gamma_l^d}$ due to van der Waals attractions between the solid and liquid. Summing these forces gives

$$\gamma_s - \sqrt{\gamma_s^d \gamma_l^d} \tag{6}$$

The total force of interaction thus becomes

$$\gamma_{sl} = \gamma_l + \gamma_s - 2\sqrt{\gamma_l^d \gamma_s^d} \tag{7}$$

Substitution of this expression into Young's equation yields

$$\cos \theta = 2\sqrt{\gamma_s^d \gamma_l^d / \gamma_l} - 1 \tag{8}$$

This equation shows that a plot of $\cos \theta$ vs $\sqrt{\gamma_l^d / \gamma_l}$ should be linear with an intercept at (0,-1) and a slope of $2\sqrt{\gamma_s^d}$. Saito and Yabe (10) used these plots to present contact angle data of different liquid pairs on paraffin, polystyrene and polyethylene. For paraffin and polyethylene, where only dispersion forces act, the linear regression line

through the data also passed through the point (0,-1) as expected. For polystyrene, which should have a polar force component, the linear regression line did not pass through the point (0,-1). Although the data plot was linear, the fact that the regression line did not pass through the predicted intercept reinforces the assumptions that the equation is applicable when only dispersion forces are involved in the interaction.

The Fowkes equation, Eq (8), also provides the theoretical explanation of our plots of cos θ vs $1/\gamma$. Dann (21),(22) found that the dispersion component of the water-ethanol series of liquids is nearly constant (18.6±1.4 dynes/cm) for concentrations up to 90% ethanol. Taking γ_1^d as constant, Eq (8) shows that a plot of cos θ vs $1/\gamma_1$ should be linear with intercept at (0,-1) and a slope of $2\sqrt{\gamma_s^d \gamma_1^d}$. Plots for three materials are shown in Figs. 3, 4 and 5. Surface tension values for these plots are given in Table 3. Contact angle data for Paraffin are given in Table 6 which is discussed in the next section. The equations of the regression lines shown in these plots are given in Table 4.

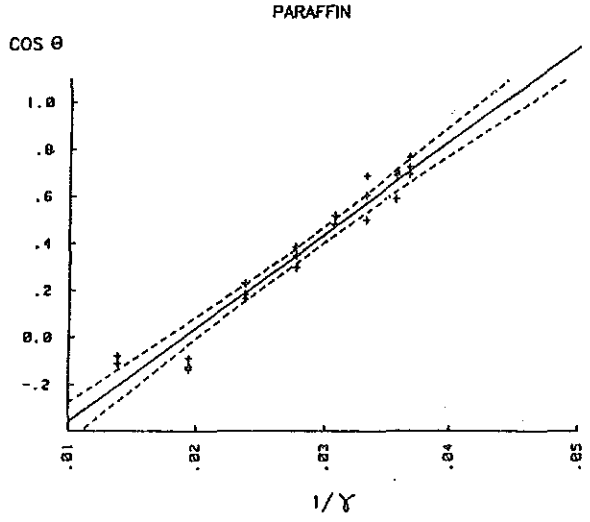

Figure 3. Plot of cosine of the contact angle, θ, vs the reciprocal of the surface tension, γ, for paraffin.

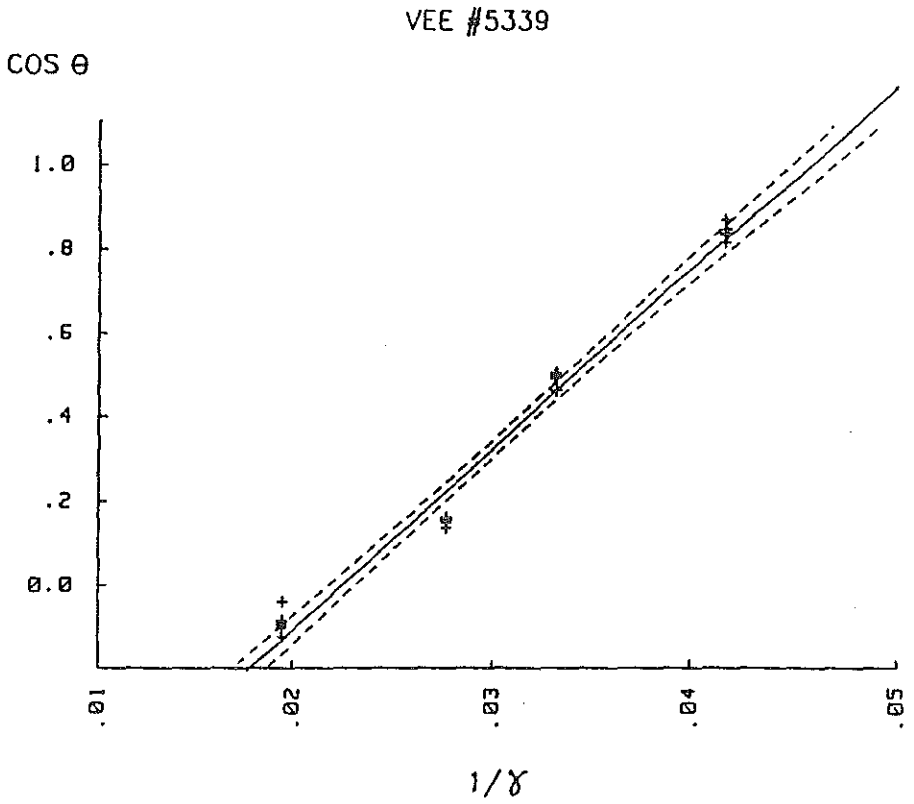

Figure 4. Plot of cos θ vs 1/γ for material 5339.

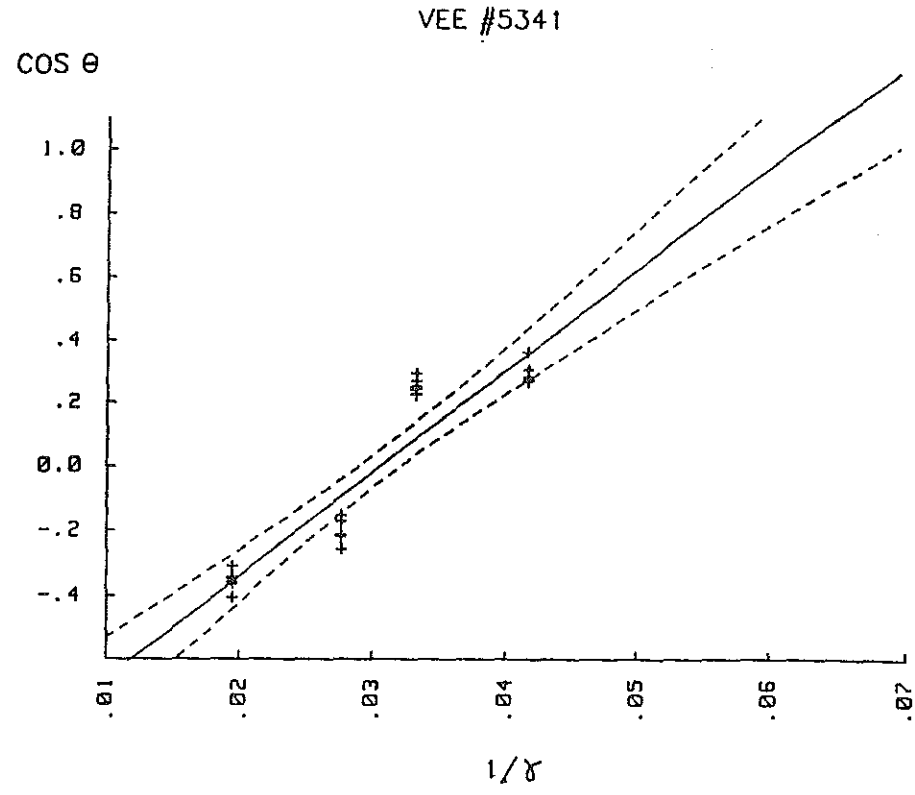

Figure 5. Plot of cos θ vs 1/γ for material 5341.

An alternative method used plots of cos Θ vs $1/\sqrt{\gamma_1}$ to analyze contact angle data and obtain the critical surface tension. These plots were based on work by Girifalco and Good (5) who treated the interfacial tensions much the same as Fowkes (8) by assuming that the interfacial attractions averaged according to the geometric mean rule. To account for possible deviations from the strict geometric mean averaging, Girifalco and Good (5) introduced the function ϕ which was expected to be system dependent and could be calculated from known (or separately measured) system properties. Eq (7) was written in the form

$$\gamma_{sl}=\gamma_s+\gamma_1- 2\phi \sqrt{\gamma_s \gamma_1} \qquad (9)$$

With this substitution for γ_{sl} in Young's equation and making the usual assumption that π_e is negligible, they obtained

$$\cos \Theta = 2\phi\sqrt{\gamma_s \gamma_1}/ \gamma_1 -1 \qquad (10)$$

For regular systems, $\phi = 1$ and for many other systems ϕ is close to unity (5). Assuming $\phi = 1$, Eq (10) becomes

$$\cos \Theta = 2\sqrt{\gamma_s/\gamma_1} -1 \qquad (11)$$

This shows that plots of cos Θ vs $1/\sqrt{\gamma_1}$ should be linear with intercept at (0,-1) and a slope of $2\sqrt{\gamma_s}$. Figures 6, 7, and 8 show these plots to be nearly as linear as the graphs of cos Θ vs $1/\gamma$ (Figs. 3, 4, and 5). Regression equations for the data in Figs. 6, 7, and 8 are given in Table 4. The r^2 values in Table 4 verify the linearity of both plots

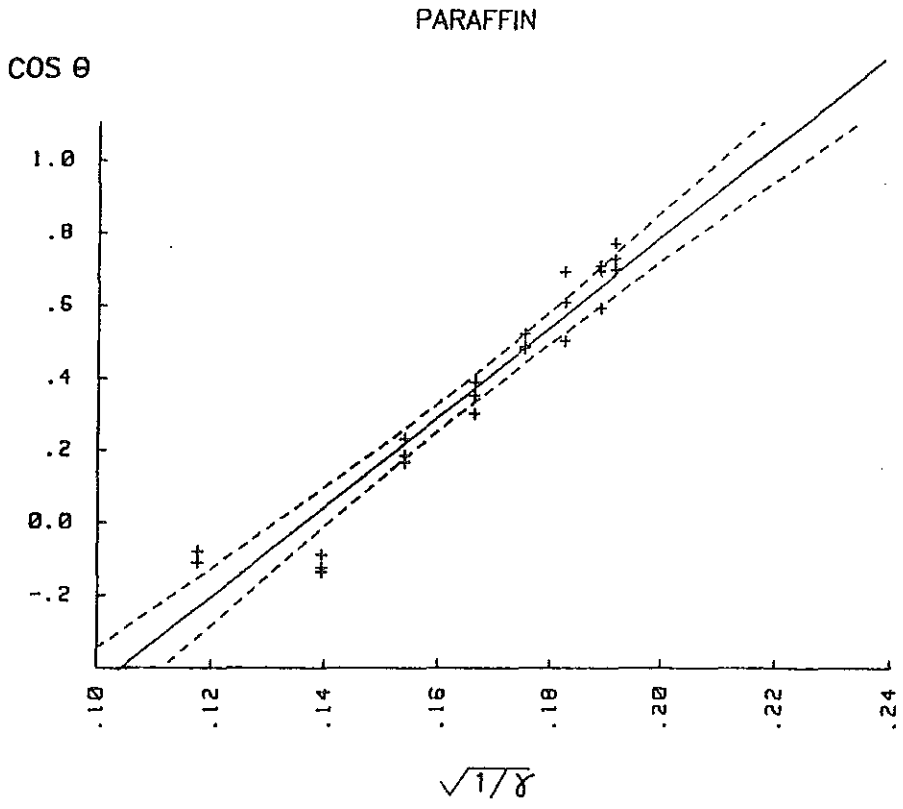

Figure 6. Plot of cos θ vs 1/γ for paraffin.

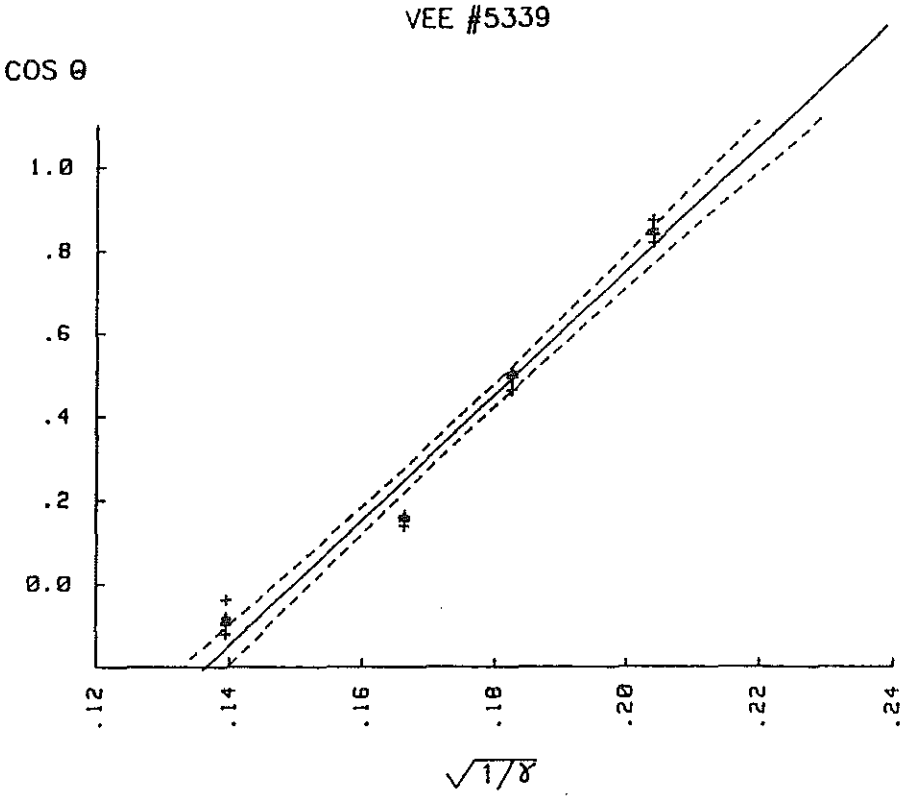

Figure 7. Plot of cos θ vs 1/γ for material 5339.

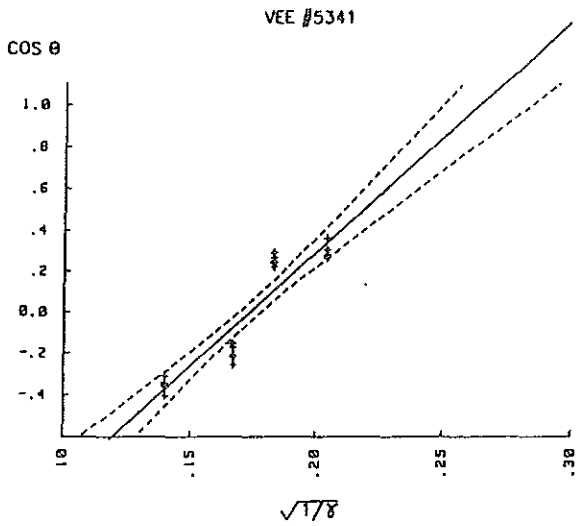

Figure 8. Plot of cos θ vs 1/γ for material 5341.

Table 4. Linear Regression Equations for Materials Evaluated

MATERIAL	EQUATION	r^2
VEE 5339	COS θ = -Ø.97+42.97/γ	Ø.983
	COS θ = -2.19+14.67/$\sqrt{\gamma}$	Ø.969
VEE 534Ø	COS θ = -Ø.92+37.Ø5/γ	Ø.978
	COS θ = -1.93+12.44/$\sqrt{\gamma}$	Ø.976
VEE 5341	COS θ = -Ø.98+32.19/γ	Ø.856
	COS θ = -1.93+11.12/$\sqrt{\gamma}$	Ø.866
VEE 5342	COS θ = -Ø.67+32.74/γ	Ø.986
	COS θ = -1.63+11.33/$\sqrt{\gamma}$	Ø.992
VEE 5382	COS θ = -Ø.26+3Ø.22/γ	Ø.893
	COS θ = -O.87+8.66/$\sqrt{\gamma}$	Ø.917
VEE 5383	COS θ = -Ø.45+29.88/γ	Ø.98Ø
	COS θ = -1.29+1Ø.15/$\sqrt{\gamma}$	Ø.979
VEE 5384	COS θ = -1.31+46.28/γ	Ø.959
	COS θ = -2.66+15.94/$\sqrt{\gamma}$	Ø.941
VEE 5385	COS θ = -Ø.35+29.Ø6/γ	Ø.969
	COS θ = -1.17+9.82/$\sqrt{\gamma}$	Ø.956
PARAFFIN	COS θ = -Ø.76+39.98/γ	Ø.944
	COS θ = -1.69+12.4Ø/$\sqrt{\gamma}$	Ø.926
NYCO-QUARPEL	COS θ = -1.24+25.8Ø/γ	Ø.885
	COS θ = -1.9Ø+8.36/$\sqrt{\gamma}$	Ø.873

and show that selection of the true model cannot be made on the basis of which model statistically best fits the data. For several materials the plots of cos θ vs $1/\gamma$ have the predicted intercept of $(\emptyset,-1)$. Assuming this means they fit the model, the conclusion is that these surfaces must be nonpolar. (The model holds for nonpolar interactions and the liquids used are known to be polar). For these materials γ_c obtained by extrapolation to cos $\theta = \emptyset$ is in reasonable agreement (within 15%) of the value γ_s^d obtained from the slope of the cos θ vs $1/\gamma$ curve.

Although it is not stated, it has been claimed (7),(8) that Eq (11) applies when only dispersion forces are active. This restriction is implied undoubtedly because of the nature of the interaction term. Good (4) has modified Eq (11) to account for dipole interactions as well as induction interactions by expressing ϕ as the sum of contributions from the London (dispersion), inductive, and dipole interactions, i.e., $\phi = \phi_d + \phi_i + \phi_p$. Only two of the materials tested gave intercepts close to the values predicted by Eq (11). Even for these materials it is difficult to interpret what a fit to this equation means. If this equation also holds only for dispersive forces, the conclusion would be that the surfaces are nonpolar. However, data on these materials did not fit Eq (8) which as stated above should also hold for nonpolar surfaces. At present it appears that plots of cos θ vs $1/\gamma$ are preferred for analyzing contact angle data and for obtaining γ_c values. However, if polar forces may be present, a modification of Eq (8) to include polar attractions, i.e., the extended Fowkes or Wu equations, or the modification proposed by Good (4), must be used. These equations were not used in this effort but the analysis given by Saito and Yabe which was

based on the extended Fowkes equation was used to evaluate the data obtained on paraffin as a check to see if impurities had imparted a polar component.

As stated above, γ_c is obtained by measuring the contact angle between the fabric and a series of drops, each taken from a liquid of successively lower surface tension (lower surface tension liquids produce smaller contact angles as shown in Fig. 2). The cosine of the contact angle is plotted against the reciprocal of the surface tension, Eq (8) and the linear regression line is obtained. For those cases where data fits the model (i.e. linear and intercept (Ø, -1)) the slope provides a good value for γ_c. When the data does not fit the model the regression line must be extrapolated to $\cos \Theta = 1$ to provide γ_c.

In those cases where extrapolation was required, as often happened in our measurements, the accuracy of γ_c provided by both equations depends on the precision of the extrapolations. This means that a series of liquids must be used which (a) provide a linear plot with good correlation and (b) provide a liquid with a small enough contact angle that the extrapolation will be reasonable.

A reasonable extrapolation depends on several factors such as the desired accuracy of γ_c, degree of correlation (r^2 value), minimum contact angle, and the number of data points (N). For the data shown in Tables 4 and 5, N >2Ø (four levels times a minimum of five replications) for all materials tested and the minimum contact angle is approximately $3Ø^{O}$. Under these conditions with r^2 >Ø.92, γ_c, or at least its dispersion component, is determined to within plus or minus 12% with 95% confidence.

TABLE 5. Critical Surface Tension (γ_c) and Maximum Surface Tension for Wetting ($\gamma_{\theta = 90^o}$) Obtained from Equations (Table 4)

FABRIC	VEE#	γ_c	$\gamma_{\theta=90^o}$
Bioflex	5339	21.2 (N/cm*10^5)	44.9 (N/cm*10^5)
Dinkam 3501S	5340	18.0	41.5
Dinkam 3001	5341	14.4	33.2
Dinkam PF151	5342	18.6	48.3
Klimate	5381	N/A	N/A
Gore-Tex II	5382	21.4	99.1
Bion II	5383	19.6	61.9
Klimate (no finish)	5384	19.0	35.9
Porelle film	5385	20.5	70.4
Sympatex/NYCO	5479	N/A	N/A

From a practical point of view, there seems to be very little difference between the two assumptions regarding the dependence of cos θ vs surface tension. This is demonstrated below with data obtained on a surface of paraffin wax.

Evaluation of Method Using Paraffin

The procedures described above were used to determine the critical surface tension of a paraffin surface. Paraffin is a water repellent material often used as a standard in surface tension work. The contact angle between water and paraffin is well known. The value of 96^o obtained in this work is slightly lower than the value of 106^o given by Saito and Yabe (10).

Plots of cos θ vs $1/\gamma$ and vs $1/\sqrt{\gamma}$ for the data of Table 6 are shown in Figs. 3 and 6, respectively. Both plots show a linear relationship. Using a least squares linear regression, the data fit the cos θ vs $1/\gamma$ relationship more closely than when regressed vs $1/\sqrt{\gamma}$, but the difference is small. It should be remembered that plotting vs $1/\sqrt{\gamma}$ is preferred

according to one molecular theory. The values obtained for γ_c of paraffin are 22.7 mN/m(=dyne/cm) when using $1/\gamma$ and 21.3 mN/m for plots of $1/\sqrt{\gamma}$.

In these measurements, the data fit the linear relationship quite closely and the range of data was such that only a short extrapolation was required to reach the value of $1/\gamma$ (or $1/\sqrt{\gamma}$) for which $\cos \theta = 1$. At this value of γ, $\theta = 0$ and instant wetting or spreading of the drop would occur. This by definition is the γ_c value for the paraffin.

TABLE 6. Contact Angles for Ethanol-Water Mixtures on Paraffin

% ETHANOL	CONTACT ANGLE, DEGREES			AVERAGE
0	96.53	94.79	96.60	95.97
10	95.30	97.29	97.97	96.85
20	79.68	76.97	80.77	79.14
30	72.85	67.49	69.70	70.01
40	58.93	61.57	61.25	60.58
50	52.95	46.71	60.21	53.29
60	45.35	54.09	46.55	48.66
70	40.13	46.21	43.87	43.40

For paraffin, taking $\gamma_s^d = 24.8$, (Saito and Yabe)(10) this equation predicts a slope of 43.1 mN/m. The experimental value of 40.0 mN/m (Table 4) was in good agreement with the theory. The experimental intercept of -0.76 (instead of -1.0) was thought to have been caused by impurities in the paraffin which may have added a polar contribution without significantly altering the dispersion interactions.

As previously stated, the analysis of Saito and Yabe was used to evaluate the polar component of the paraffin used in this work. These

equations gave γ_s^d = 25.5 mN/m and γ_s^p = Ø mN/m for the data we obtained. Since pure paraffin is known to have no polar forces, γ_s^p should be zero. The zero value we obtained suggests that the paraffin used was reasonably pure. Why this data did not give the predicted intercept is not known, but it may be related to the low contact angles observed.

Measurements on Experimental Films

The above technique was applied to the experimental films listed in Table 1. Plots of cos θ vs $1/\gamma$ for two of these experimental films are shown in Figs. 4 and 5. Figure 4 shows results obtained on material VEE # 5339 and represents an ideal case. The data fit the linear relationship very well (r^2 = Ø.983) and only a short extrapolation (cos θ = Ø.7 to 1.Ø) is required to obtain γ_c. Figure 5 is a plot of data obtained on material VEE # 5341 and shows a very different situation. The data do not fit the regression curve as well (r^2 = Ø.856) and in addition, a long extrapolation (cos θ = Ø.3 to 1.Ø) is required to determine γ_c. Replacing the independent variable by $1/\sqrt{\gamma}$ does not alter the above picture. Figure 7 (VEE # 5339) again shows ideal behavior while Fig. 8 (VEE # 5341) shows a poorer fit to the data and the long extrapolation required.

The equations obtained by a least squares fit for the data shown in Figs. 4, 5, 7 and 8 are given in Table 4 along with the linear regression equations (using both $1/\gamma$ and $1/\sqrt{\gamma}$ as independent variables) for all materials evaluated, including paraffin and the Quarpel treated NYCO (Table 2). Also included in the table are the coefficients of determination, r^2. Evaluation of these equations for cos θ = 1 shows that the two theories agree within 1Ø% in most cases.

In addition to providing the γ_c value, the linear equation permits the calculation of the surface tension of that liquid which produces a contact angle of 90° when in contact with the film surface. This liquid, and all others having higher surface tension, will not wet the fabric. Data obtained from the least squares equations for the eight films evaluated are given in Table 5. These data are for equations based on plots of cos θ vs $1/\gamma$.

Measurements of Fabrics

Figure 9 shows the data obtained on the first item listed in Table 2, Nyco with Quarpel surface treatment. It is clear that this highly repellent surface cannot be accurately measured by the methods described above. The data appear to be linear but the extrapolation covers more than twice the range of data and produces a very questionable value for γ_c. Based on 95% confidence limits, γ_c lies between 5.6 and 10.5. This clearly demonstrates the uncertainty of the extrapolation.

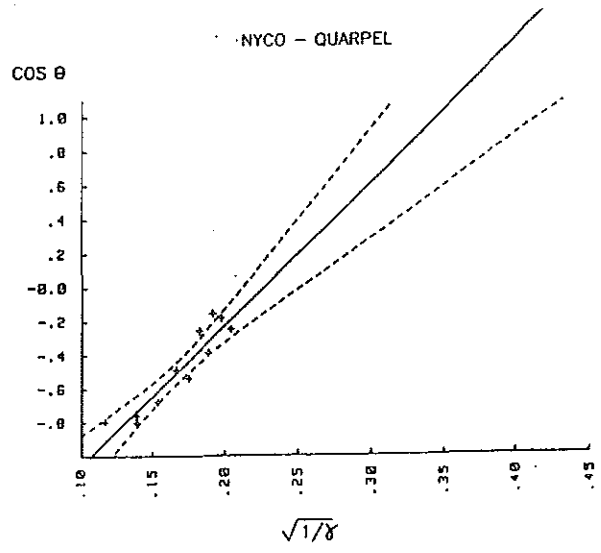

Figure 9. A plot of cos θ $1/\gamma$ for Nyco fabric with a Quarpel surface treatment.

The long extrapolation comes from the fact that all the liquids used, even the 100% ethanol with a surface tension of 24 dynes/cm, produced a very large contact angle. Several factors are believed to contribute to these high contact angles other than the true surface properties of the fibers. The surface of the fabric is very rough due primarily to the contoured pattern formed by the weaving of the yarns. Surface roughness is known to cause many difficulties in the measurement of contact angle (13-18). The fiber orientation in the fabrics produces large distortions in the three phase line (contact line where the fabric, the liquid, and the vapor saturated air all meet) as shown in Fig. 10. The ridges cause variations in the contact angle which results in crimping or a bottle-cap effect. The measurement of a contact angle is meaningless on a small scale such as that represented in Fig. 10 due to the large changes in value over small spatial distances. On a larger scale where these fine details cannot be observed, an average contact angle can be measured. As mentioned previously, even on this larger scale, the contact angle may depend strongly on orientation of the fibers requiring measurements along two mutually perpendicular axes.

Figure 10. An enlargement of an ethanol-water drop on a fabric. Irregularities in the contact line "bottle cap effect") are due to the surface roughness.

In addition to roughness causing potential bias in contact angles, it might very well permit air to be trapped between the deposited drop and the fabric. This of course would keep the drop from making good contact with the fabric and give an apparent contact angle much higher than would be obtained on a smooth surface (28),(29). A third potential source of high contact angles is the small fibrils that protrude from the woven yarns. These fibrils can often be seen propping up the drop in one or more locations. This too would tend to increase the contact angle. These factors, either singly or in combination, undoubtedly increase the contact angle for rough fabrics above that for the same surface treatment on a smooth surface. From these observations, it is clear that an approach based on the measurement of contact angles for different surface tension liquids is not suitable for the highly repellent rough surfaces of fabrics that are of greatest military interest.

Present Efforts

The failure of the above method to provide accurate γ_c values for low surface energy materials that are of primary interest in developing water resistant fabrics indicated the need for alternative measures of wetting potential. Some of the difficulties encountered with the method are due to a fundamental limitation, i.e., low surface energy materials will always require long extrapolations. Because of this, totally new approaches were initiated.

The first alternative considered was to measure the time required for a liquid to break through the fabric. The time of breakthrough was detected electronically, first by mounting electrodes above and below the fabric and measuring the resistance change when the fabric wet and made a

low resistance liquid path to the second electrode. Data obtained showed much scatter in the breakthrough times. It was thought that the small DC current required to obtain resistance data might be affecting the surface charge on the fabric. These induced surface charges could affect the wetting characteristics of the fabric and thus produce the observed scatter.

The method of monitoring breakthrough was modified by placing both electrodes on the same side of the fabric. The electrodes were mounted side by side and separated by approximately Ø.5 mm. As a drop penetrated through the fabric, a liquid bridge across the Ø.5-mm gap would lower the continuously monitored electrical resistance between the electrodes. By measuring the breakthrough times for a series of liquids of differing surface tension, it was thought that an extrapolation to a breakthrough time of Ø would indicate the surface tension of a liquid that would spread instantly. However, because of minor problems with forcing the wetting to occur over the electrode and the probability that long extrapolations similar to those of the contact angle process might be required, we decided to focus on the following methods of quantifying the wetting potential of a fabric. Present efforts concentrate on the careful measurement of the hydrostatic pressure resistance, and the flow conditions for both liquids and vapors as a function of the pressure drop across the fabric. Data obtained thus far are reproducible and agree reasonably well with appropriate theory. These data will be applied to various models in the hope that parameters describing the wetting potential of the cloth will be identified.

CONCLUSIONS

1. Instrumental methodology has been established which permits the measurement of the angles of contact between most liquids and relatively smooth surfaces. Apparent contact angles for many rough surfaces can also be measured and if desired a detailed picture of the three-phase line can be obtained. The method will also work for single fibers.

2. Using contact angle data for liquids of different surface tension, the critical surface tension can be determined for most smooth surfaces.

3. We believe the contact angle method has a fundamental limitation which prevents the accurate determination of critical surface tension for highly water repellent (low surface energy) fabrics and films. Low energy materials require long extrapolations to obtain γ_c. Since the extrapolations are based on uncertain models ($1/\gamma$ vs $1/\sqrt{\gamma}$), reliability is greatly reduced. Other parameters and measurements not involving the determination of a contact angle are needed to quantify the wetting potential of these materials.

4. For most smooth surfaces, analysis of contact angle data using plots of $\cos\theta$ vs $1/\gamma$ (Fowkes) or vs $1/\sqrt{\gamma}$ (Good) provide essentially the same results. Both plots appear equally linear over the data range obtained and require similar extrapolations.

5. Methodology has been established for the measurement of the surface tension of most liquids.

6. Present efforts show promise of providing a reliable measure of the wetting potential of water resistant materials.

FUTURE EFFORTS

It is clear from these findings that the determination of the wetting potential of highly repellent rough fabrics requires one or more new approaches. In addition to continuing the present efforts described above, other avenues to consider include use of indirect methods of measuring contact angles such as surface tension forces on a strip of material immersed in a liquid and an improvement of the method (described earlier) for measuring the breakthrough time. The first of these methods would have some drawbacks, particularly for materials treated only on one surface.

If it becomes possible to make an accurate measurement of a contact angle on a rough fabric surface, further studies of the theories based on molecular mechanics (the extended Fowkes equation and the Φ-function proposed by Good and coworkers) should be undertaken. These approaches provide a means of calculating the critical surface tension of a fabric from only one or two measured contact angles.

It would also be worthwhile to determine the significance of the slope of the curves of $\cos \theta$ vs $1/\gamma$ (Fowkes model) or $\cos \theta$ vs $1/\sqrt{\gamma}$ (Good model). Depending on the model chosen, this slope could provide desired data on the polar and dispersion components of the surface tension of the test material.

It might also be profitable to study in detail the theories dealing with surface roughness. The effective contact angle described by Cassie and Baxter (28) could be critical to understanding the liquid repellency of breathable fabrics.

Methods based on Molecular mechanics, in combination with models describing the effects of surface roughness and empirical measurements of hydrostatic pressure resistance and flow rates should provide the necessary information to accurately predict the wetting characteristics of nearly all fabrics and films.

REFERENCES

1. Zisman, W.A., Relation of the Equilibrium Contact Angle to Liquid and Solid Constitution, Advances in Chemistry, 43: Contact Angle, Wettability and Adhesion, 1-51, 1964.

2. Fox, H.W. and W.A. Zisman, The Spreading of Liquids on Low Energy Surfaces. I. Polytetrafluoroethylene. J. Colloid Sci., 5, 514-531, 1950.

3. Zisman, W.A., Influence of Constitution on Adhesion. Ind. Eng. Chem., 55, 10, 19-38, 1963.

4. Good, R.J., Surface Free Energy of Solides and Liquids: Thermodynamics, Molecular Forces, and Structure. J. Colloid Interface Sci., 59, 398-419, 1977.

5. Girifalco, L.A. and R.J. Good, A Theory for the Estimation of Surface and Interfacial Energies. I. Derivation and Application to Interfacial Tension. J. Phys. Chem., 61, 904-909, 1957.

6. Good, R.J., Theory for the Estimation of Surface and Interfacial Energies. VI. Surface Energies of some Fluorocarbon Surfaces from Contact Angle Measurements, Advances in Chemistry, 43: Contact Angle, Wettability and Adhesion, 74-87, 1964.

7. Fowkes, F.M., Determinations of Interfacial Tensions, Contact Angles and Dispersion Forces in Surfaces by Assuming Additivity of Intermolecular Interactions in Surfaces. J. Phys. Chem., 66, 382, 1962.

8. Fowkes, F.M., Attractive Forces at Interfaces. Ind. and Eng. Chem., 56, 40-52, 1964.

9. Owens, D.K. and R.C. Wendt, Estimation of the Surface Free Energy of Polymers. J. Applied Polymer Sci., 13, 1741-1747, 1969.

10. Saito, M. and A. Yabe, Dispersion and Polar Force Components of Surface Tension of Some Polymer Films. Textile Research Journal, 53, 54-59, 1983.

11. Wu, S., Calculation of Interfacial Tension in Polymer Systems. J. Polymer Sci.: Part C, 34, 19-30, 1971.

12. Yuk, S.H. and M.S. Jhon, Contact Angles on Deformable Solids. J. Colloid and Interface Sci., 110, 252-257, 1986.

13. Dettre, R.H. and R.E. Johnson, The Spreading of Molten Polymers. J. Adhesion, 2, 61-63, 1970.

14. Oliver, J.F. and S.G. Mason, Liquid Spreading on Rough Metal Surfaces. J. Materials Sci., 15, 431-437, 1980.

15. Huh, C. and S.G. Mason, Effects of Surface Roughness on Wetting (Theoretical). J. Colloid Interface Sci., 60, 11-38, 1977.

16. Carroll, B.J., The Equilibrium of Liquid Drops on Smooth and Rough Circular Cylinders. J. Colloid Interface Sci., 97,

17. Shuttleworth, R. and G.L.J. Bailey, The Spreading of a Liquid Over a Rough Solid. Disc. Farad. Soc., 3, 16-22, 1948.

18. Cox, R.G., The Spreading of a Liquid on a Rough Solid Surface. J. Fluid Mech., 131, 1-26, 1983.

19. de Gennes, P.G., Wetting: Statics and Dynamics. Rev. Modern Phys., 57, 827-863, 1985.

20. Cowsar, D.R. and L.M. Speaker, Interaction of Liquid Jets and Sprays with Supported Films and Drops: Substrate Characterization. Chemical Systems Lab Report, ARCSL-CR-82032, Southern Research Institute, pp. 151, 1982.

21. Dann, J.R., Forces Involved in the Adhesive Process. I. Critical Surface Tensions of Polymeric Solids as Determined with Polar Liquids. J. Colloid and Interface Sci., 32, 302-320, 1970.

22. Dann, J.R., Forces Involved in the Adhesive Process. II. Nondispersion Forces at Solid-Liquid Interfaces. J. Colloid and Interface Sci., 32, 321-331, 1970.

23. Graham, D.P., Physical Adsorption on Low Energy Solids. II. Adsorption of Nitrogen, Argon, Carbon Tetrafluoride and Ethane on Polypropylene. J. Phys. Chem., 68, 2788-2792, 1964.

24. Graham, D.P., Physical Adsorption on Low Energy Solids, III. Adsorption of Ethane, N-Butane, and N-Octane on Poly(tetrafluoroethylene).

25. Wade, W.H. and J.W. Whalen, Pendular-Ring Condensation on Teflon Powders. J. Phys. Chem., 72, 2898-2902, 1968.

26. Whalen, J.W., Adsorption on Low-Energy Surfaces: Hexane and Octane Adsorption on Polytetrafluoroethylene. J. Colloid Interface Sci., 28, 443-448, 1968.

27. Good, R.J., Spreading Pressure and Contact Angle. J. Colloid Interface Sci., 52, 308-313, 1975.

28. Cassie, A.B.D. and S. Baxter, Wettability of Porous Surfaces. Trans. Faraday Soc., 40, 545-551, 1944.

29. Cassie, A.B.D., Contact Angles. Discuss. Faraday Soc., 3, 11-16, 1948.